

POLYVINYLIDENE FLUORIDE BASED NANOCOMPOSITES WITH HIGH DIELECTRIC CONSTANT

ShuQin Li^{*}, JingWen Wang, Jun Xiao

College of Materials Science and Technology, Nanjing University of Aeronautics and Astronautics,
No.29, YuDao Street, Nanjing, Jiangsu Province, China

*shuqli@nuaa.edu.cn

Keywords: Nanocomposites, Dielectric constant, Carbon nanotubes, Polyvinylidene fluoride

Abstract

PVDF based nanocomposites filled by unmodified multi-walled carbon nanotubes (U-MWCNTs), acid treated multi-walled carbon nanotubes (A-MWCNTs) and TETA modified of multi-walled carbon nanotubes (TETA-MWCNTs) were prepared by the solution cast method. The FTIR spectra confirm that multi-walled carbon nanotubes were successfully modified by acid and triethylene-tetramine. The comparison of Raman spectra of the U-MWCNTs, A-MWCNTs and TETA-MWCNTs mean that modification of the MWCNTs does not affect the graphite structure of the MWCNTs. The FESEM images prove that the dispersibility of A-MWCNTs and TETA-MWCNTs in PVDF matrix was remarkably improved. From the analysis of dielectric properties of PVDF nanocomposites enhanced by MWCNTs, it is concluded that modification of MWCNTs for good compatibility with PVDF matrix is essential for attractive high dielectric constant nanocomposites.

1. Introduction

Multi-walled carbon nanotubes (MWCNTs) have attracted scientific and technological interest worldwide since the discovery of MWCNTs by Iijima [1]. Polyvinylidene fluoride (PVDF) based composites with high dielectric constant have also aroused great attention for their important technological applications such as electronic packaging and components, electromechanical devices, high performance capacitor and electric energy storage devices [2-5]. However, the dielectric constant of PVDF is far lower than that of inorganic ceramic or metal particulates. In the past, several works for increasing the dielectric permittivity by filling some high dielectric constant ceramic powders into the polymers had been done [6-8]. MWCNTs with high aspect ratio and unique physical properties, in particular, electrical and mechanical properties can also be used as excellent filler in the same way [9]. Dr. Wang etc. have studied PVDF nanocomposites filled by MWCNTs with high dielectric constant and concluded that the dielectric properties of MWCNTs/PVDF nanocomposites may be improved without the chemical functionalization to the carbon nanotubes further [10]. But the dispersion of MWCNTs in the polymers is rather poor due to their incompatibility with polymers and large surface-to-volume ratio, which will affect the dielectric properties as well as the processability of nanocomposites [11,12]. Therefore, surface modification to MWCNTs is needed in order to improve the dispersion of MWCNTs in the polymeric matrix [13,14]. In this paper, surface treatment of MWCNTs by

concentrated acid is carried out, PVDF based nanocomposites filled by MWCNTs are prepared, the morphologies of fractured surface of the MWCNTs/PVDF nanocomposites are characterized by FESEM, and the dielectric constant of the nanocomposites are measured and analyzed.

1.1. Materials

MWCNTs were prepared by a chemical vapor deposition method with a purity of carbon content more than 95vol% (supplied by Shenzhen Nanotechnologies Port Co.). The diameter of the MWCNTs was 40–60 nm and the length was 5-15 μ m, the specific surface area was 40-300 m²/g and the content of amorphous carbon was 2%. The acid modified MWCNTs (A-MWCNTs) and the TETA modified MWCNTs (TETA-MWCNTs) were obtained from the methods as reference[16]. Polyvinylidene fluoride (PVDF) with a weight-averaged molecular weight of 400,000 was obtained from Shanghai 3F Company, China. N,N-dimethylformamide (DMF) of analytical grade was dried with CaH₂ followed by distillation in vacuo prior to use. Concentrated sulfuric acid (H₂SO₄≥95.98%), nitric acid (HNO₃=65.68%) and other reagents and solvents were obtained from Shanghai Chemical Reagent Co.

1.2. Preparation of MWCNTs/PVDF Nanocomposites

U-MWCNTs/PVDF and A-MWCNTs/PVDF nanocomposites were both prepared using the solution cast method [3]. The PVDF was dissolved in DMF and then a proper amount of MWCNTs were added to the solution. The solution was ultrasonically stirred until the MWCNTs were dispersed. Afterward, the solution was poured onto a glass slide and dried in air at 70°C for 5 h, then under vacuum at 70 °C for 12 h. Finally, the composites were annealed at 140°C in a vacuum for 12 h and slowly cooled to room temperature. The MWCNTs/PVDF composite films were obtained. The typical film thickness is about 40 μ m-60 μ m. For the electric characterization, the films were cut into small pieces of 10×10 mm, and circular Aluminium electrodes with 2.5 mm radius were sputtered in the center on both surfaces of each sample.

1.3. Characterization

FTIR spectra of U-MWCNTs and A-MWCNTs were recorded with a Bruker Vector-22 Fourier-transform infrared (FTIR) spectrometer. The samples were pressed into a tablet with potassium bromide (KBr) separately. The MWCNTs were also characterized with a JY – T64000 Raman spectroscopy. The morphologies of the fractured surface of MWCNTs/PVDF nanocomposites were observed by field emission scanning electron microscopy (FESEM) (LEO 1550). The samples were broken in liquid nitrogen and the fractured surfaces of nanocomposites were coated with conductive gold paint by vacuum sputtering. For the characterization of the dielectric properties of MWCNTs/PVDF nanocomposites in the frequency range from 100 Hz to 10 MHz at room temperature, an Agilent 4194A Impedance analyzer was used, and the dielectric constant K of the composite films was calculated by the formula according to reference.

2. Results and discussion

In order to characterize the MWCNTs treated chemically with concentrated acid, we measured the FTIR spectrum shown in Fig.1. In Fig.1(a), which is for the U-MWCNTs, the

feature at wavenumbers 3000-2800 cm^{-1} corresponds to -CH stretching and that at 3402 cm^{-1} corresponds to -OH stretching. The FTIR result (-CH stretching) indicates that U-MWCNTs contain defects, which may be formed during their manufacture [15]. Fig.1(b) presents the FTIR spectrum of A-MWCNTs: carboxylic groups stretching (COOH) appears at 1724 cm^{-1} . Features at wavenumbers 1610-1550 cm^{-1} , 3000-2800 cm^{-1} and 3650-3000 cm^{-1} are the absorption peaks of COO^- symmetric stretching, -CH stretching and $-\text{COO}^-$ stretching, respectively. The FTIR spectra confirm that carboxylic groups have been introduced to the MWCNTs successfully by acid treatment.

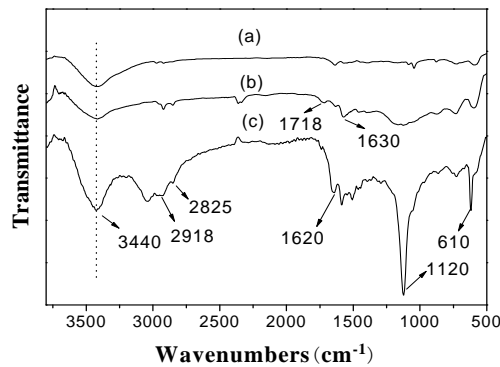


Figure 1. FTIR spectra of (a) U-MWCNTs, (b) A-MWCNTs and (c) TETA-MWCNTs

The Raman spectrum of the U-MWCNTs and A-MWCNTs are shown in Fig.2. From the Raman spectra we know that the spectra of the U-MWCNTs and A-MWCNTs are very similar, they have the same pattern. That mean that acid treatment of the MWCNTs does not affect the graphite structure of the MWCNTs. The presence of the two broad bands at 1,350 cm^{-1} and 1,580 cm^{-1} , usually referred as to D (disorder, sp^3 banding) and G (graphitic, sp^2 banded carbon) bands. The value of intensity ratio between the G- and D-bands (IG/ID) serves as a measure of the graphitic ordering and indicates the approximate crystalline size in the hexagonal plane. Comparing the IG/ID ratios of the samples, which are 1.24 for U-MWCNTs and 1.06 for A-MWCNTs, reveals that acid treatment of U-MWCNTs increases defects scattering on sidewall of nanotubes [16].

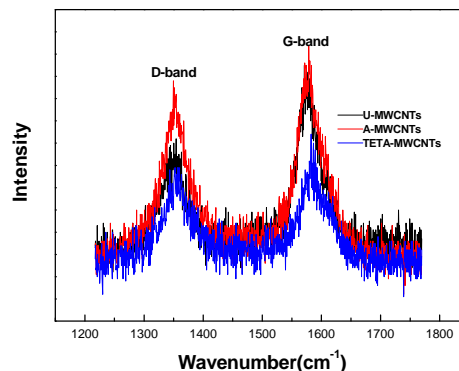
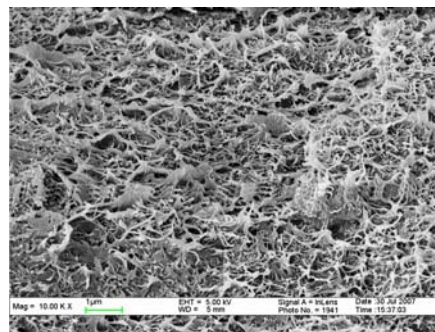


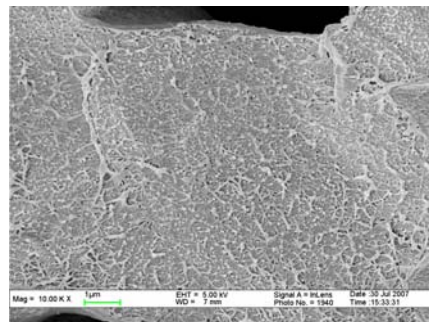
Figure 2. Ramam spectra of U-MWCNTs, A-MWCNTs and TETA-MWCNTs

FESEM morphologies of the fractured surface of MWCNTs/PVDF nanocomposites before and after acid treatment of MWCNTs are shown in Fig.3. From Fig. 3(a) we can observe that

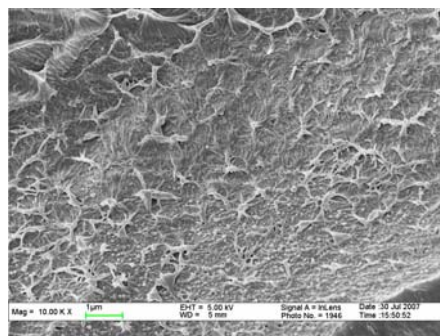
the interface of the conductive U-MWCNTs and insulate PVDF matrix is clear, and many extraction carbon nanotubes appear at the fractured surface of U-MWCNTs/PVDF nanocomposites. On the contrary, it can be seen from Fig. 3(b) that A-MWCNTs can disperse uniformly in the PVDF matrix and the interface between nanotube filler and matrix is fuzzy. This is caused by the polar groups introduced to the surface of the A-MWCNTs, which lead to good compatibility of A-MWCNTs with PVDF matrix. Furthermore, it also indicates that the A-MWCNTs may connect with each other in part, when the volume fraction of A-MWCNTs is near the percolation threshold, the electrical conducting phase may form a continuous random networks [17]. This continuous percolation networks formed by self-connecting of A-MWCNTs can play an important role on the dielectric properties of nanocomposites [18].



(a) U-MWCNTs/PVDF



(b) A-MWCNTs/PVDF



(c) TETA-MWCNTs/PVDF

Figure 3. FESEM of the fractured surface of MWCNTs/PVDF nanocomposites

Fig.4 is the dielectric properties of U-MWCNTs/PVDF and A-MWCNTs/PVDF nanocomposites at room temperature. Fig.4(a) and 4(b) reflect the dielectric constant at 100Hz of U-MWCNTs/PVDF and A-MWCNTs/PVDF nanocomposites as a function of the volume fraction of MWCNTs respectively.

The dielectric constants of the U-MWCNTs/PVDF and A-MWCNTs/PVDF nanocomposites both can follow the universality of the percolation theory. The dielectric constants of the U-MWCNTs/PVDF and A-MWCNTs/PVDF nanocomposites change very small before the percolation threshold, but increase sharply when the volume fraction of filler is near upon the percolation threshold. Percolation theory predicts that the dielectric constant K of a composite consisting of a conductive filler embedded in an insulation matrix of dielectric constant K_m is given by the following formula:

$$K = K_m \left(\frac{f_c - f}{f_c} \right)^{-q} \quad (1)$$

Where f is the volume fraction of the conductive phase, f_c is the percolation threshold of conduction, and q is a critical exponent [19,20]. Formula (1) indicates that as f approaches f_c , a large dielectric enhancement can be obtained [21]. The best fit of the dielectric constant data of U-MWCNTs/PVDF nanocomposites yield $f_c \approx 0.018$, $q \approx 0.86$ using formula (1), while the fit values of A-MWCNTs/PVDF nanocomposites are $f_c \approx 0.035$, $q \approx 1.90$. The common value of the percolation threshold is $f_c \approx 0.16$, obtained in two-phase random composites when the conducting fillers with micron scale and sphere shape are used [22]. Whereas, the percolation threshold of the U-MWCNTs/PVDF nanocomposites is only one tenth of that of common two-phase random composites. The quite low percolation threshold of the U-MWCNTs/PVDF composites is resulted from the large aspect ratio and the high conductivity of U-MWCNTs. It is noticed that the percolation threshold of A-MWCNTs/PVDF is almost equal to twice of the percolation threshold of U-MWCNTs/PVDF composites. The shortened length of A-MWCNTs due to acid treatment of MWCNTs can explain for the larger percolation threshold of A-MWCNTs/PVDF nanocomposites. Even so, the percolation threshold of the A-MWCNTs/PVDF nanocomposites is merely one fifth of that of the common two-phase random composites. The extremely low percolation can guarantee good flexibility and easy processing of the PVDF based nanocomposites. Meanwhile, giant enhancement of the dielectric constant of the nanocomposites on 100 Hz close to their percolation threshold can be observed as expected. The dielectric constant of U-MWCNTs/PVDF and A-MWCNTs/PVDF reach 1258 and 7419 at their percolation threshold, which are 146 times and 862 times of that of PVDF matrix separately. Such large dielectric constants of nanocomposites are correlated to the formation of grain boundary barrier layers and interfacial polarization and percolation effects [23-25]. The giant dielectric constant could also be attributed to Maxwell-Wagner-Sillars (MWS) space charge polarization mechanism [26,27], which exists in the composites having large differences in both the dielectric constant and conductivity between the nanotube filler and polymer matrix at low frequency. It is worth noting that the dielectric constant of A-MWCNTs/PVDF nanocomposites is about six times of that of U-MWCNTs/PVDF nanocomposites at percolation. This can be explained that uniformly dispersion of A-MWCNTs in PVDF matrix have a great effect on their physical properties of nanocomposites, and the dielectric behavior can be often suggested by the inverse Swiss-cheese model [17]. Furthermore, the results also confirm that most A-MWCNTs can become self-connected to form a continuous percolation networks at a critical volume fraction of MWCNTs. The microstructure of networks plays a crucial role in

improving the dielectric constant of composites and these networks can act as many micro-capacitors [28,29]. A complex microstructure of A-MWCNTs/PVDF is made of A-MWCNTs conducting fillers embedded in the PVDF insulating matrix when the load of MWCNTs is in the neighborhood of the percolation threshold, as a result of the migration distance of free electrons of A-MWCNTs is wider than that of U-MWCNTs. So the A-MWCNTs/PVDF nanocomposites have an extremely high dielectric constant. As for the critical exponents, $q \approx 1.90$ in A-MWCNTs/PVDF nanocomposites, are coincided with that of the universal values, which is $q = 1.6-2.0$ for dimensionality $D=3$ [30].

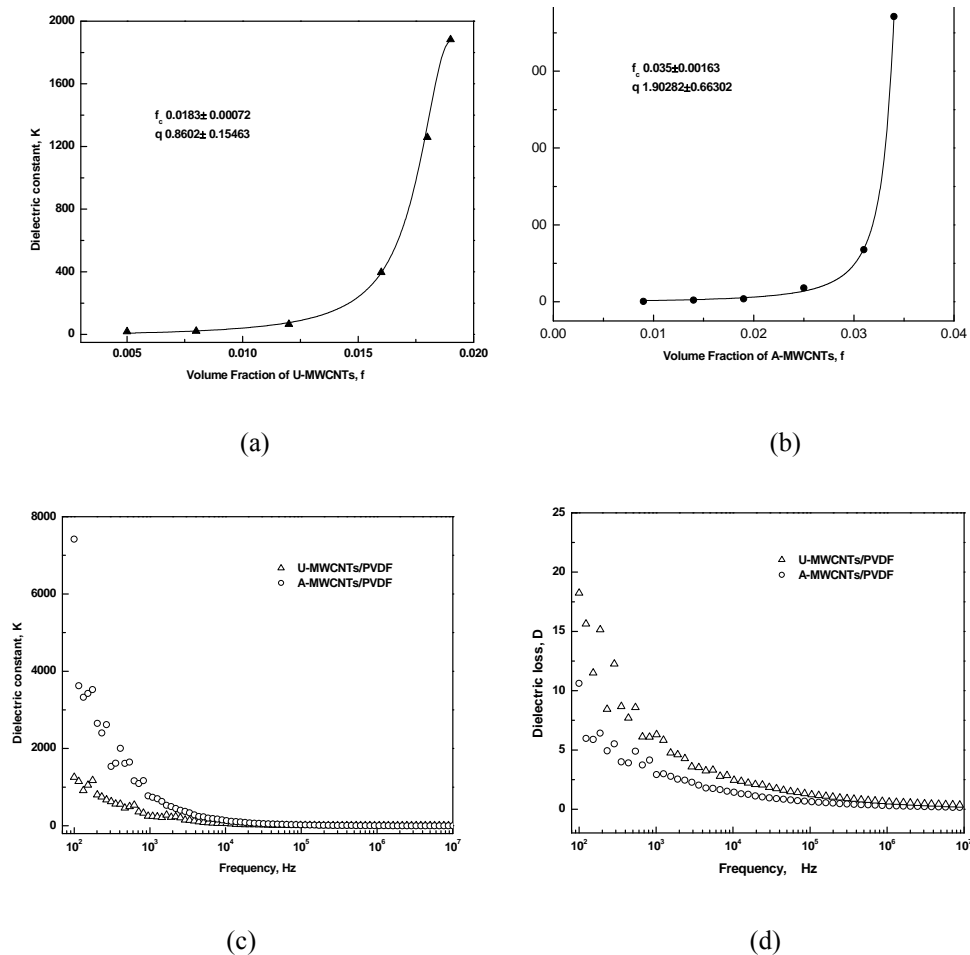


Figure 4. Dependence of the dielectric constant at 100 Hz of the nanocomposites on the volume fraction of nanotube filler: (a) U-MWCNTs/PVDF; (b) A-MWCNTs/PVDF; Dielectric dispersion of the A-MWCNTs/PVDF and U-MWCNTs/PVDF nanocomposites at percolation threshold: (c) dependence of the dielectric constant; (d) dependence of the dielectric loss on frequency.

Dependence of the dielectric constant of the A-MWCNTs/PVDF and U-MWCNTs/PVDF nanocomposites at percolation threshold on frequency is shown in Fig.4(c). The dielectric constant is of weak frequency dependent for the lower volume fraction of MWCNTs. At the same time in low frequency (10^2-10^4 Hz), the dielectric constants of the nanocomposites decrease rapidly with increasing frequency for the higher volume fraction of MWCNTs. The low-frequency dielectric dispersion could be ascribed to two factors: one factor is the Maxwell-Wagner-Sillars (MWS) space charge polarization phenomenon at low frequency; the other is the nonuniform distribution of electric field originated from a greater amount of

conductor filler added in polymer matrix.²⁹ These two factors both lead to strong dependence of the dielectric properties of nanocomposites on low frequency range.

Fig.4(d) compares the dielectric loss of A-MWCNTs/PVDF with that of U-MWCNTs/PVDF nanocomposites at their percolation thresholds. The dielectric loss of A-MWCNTs/PVDF decreases to about a half of that of U-MWCNTs/PVDF nanocomposites on the frequency of 100Hz. The dielectric loss decrease of A-MWCNTs/PVDF nanocomposites also can be ascribed to the good compatibility of A-MWCNTs with PVDF matrix. Although the dielectric loss of the A-MWCNTs/PVDF is still high, a much lower dielectric loss will be expected through the improvement of fabrication method of nanocomposites.

3.Conclusions

In order to improve the compatibility of MWCNTs with PVDF matrix, acid treatment of MWCNTs was carried out. The appearance of 1724cm^{-1} absorption peak of the FTIR spectra confirms that the MWCNTs were successfully modified by acid. The Raman spectra shows that acid treatment of the MWCNTs does not affect the graphite structure of the MWCNTs. FESEM morphologies of the fractured surface of MWCNTs/PVDF nanocomposites prove that the dispersibility of MWCNTs is remarkably improved after the acid treatment, and A-MWCNTs may connect with each other to form continuous percolation networks. The percolation thresholds of U-MWCNTs/PVDF and A-MWCNTs/PVDF are much lower than the common value. The quite low percolation threshold of the MWCNTs/PVDF composites is resulted from the large aspect ratio and the high conductivity of MWCNTs. The dielectric constant of U-MWCNTs/PVDF and A-MWCNTs/PVDF reach 1258 and 7419 at their percolation thresholds, which are 146 times and 862 times of that of PVDF matrix separately. Such large dielectric constants of nanocomposites are correlated to the formation of giant boundary barrier layers and interfacial polarization and percolation effects. The dielectric constant of U-MWCNTs/PVDF nanocomposites is much lower than that of A-MWCNTs/PVDF nanocomposites. The good dispersibility of A-MWCNTs in PVDF matrix and the microstructure of A-MWCNTs have a great effect on the giant increase of the dielectric constant of A-MWCNTs/PVDF nanocomposites. The dielectric loss of A-MWCNTs/PVDF decreases to about a half of that of U-MWCNTs/PVDF nanocomposites on the frequency of 100Hz. These all experimental data demonstrate that good compatibility of MWCNTs with in PVDF matrix is essential for attractive high dielectric constant nanocomposites. However, in order to attain ideal dielectric properties of nanocomposites for the electronic applications, it is meaningful to do some further study on preparation of the MWCNTs/PVDF nanocomposites.

References

- [1] S.C. Tjong. Structural and mechanical properties of polymer nanocomposites. *Mater Sci Eng R* (53): 73-197, 2006.
- [2] QM. Zhang, HF. Li, M.Poh, HS. Xu, ZY. Cheng, F. Xia, C. Huang. An all-organic composite actuator material with a high dielectric constant. *Nature* (419):284-286, 2002.
- [3] JW. Wang, QD. Shen, CZ. Yang, QM. Zhang. High dielectric constant composite of p(vdf-trfe) with grafted copper phthalocyanine oligomer. *Macromolecules* (37):2294-2298, 2004.
- [4] C.Huang, QM. Zhang. Fully functionalized high-dielectric-constant nanophase polymers with high electromechanical response. *Adv Mater* (17):1153-1158, 2005.
- [5] N.Levi, R.Czerw, SY. Xing, P. Iyer, DL. Carroll. Properties of polyvinylidene difluoride-carbon nanotube blends. *Nano Lett* (4):1267-1271, 2004.

- [6] ZM. Dang, YH. Lin, CW. Nan. Novel ferroelectric polymer composites with high dielectric constant. *Adv Mater* 15:1625-1629, 2003.
- [7] E. Venkatragavaraj, B. Satish, PR. Vinod, MS. Vijaya. Piezoelectric properties of ferroelectric PZT-polymer composites. *J Phys D: Appl Phys* (34):487-492, 2001.
- [8] P. Murugaraj, D. Mainwaring, N. Mora-Huertas. Dielectric enhancement in polymer-nanoparticle composites through interphase polarizability. *J Appl Phys* (98):054304, 2005.
- [9] JKW. Sandler, JE. Kirk, IA. Kinloch, MSP. Shaffer, AH. Windle. Ultra-low electrical percolation threshold in carbon-nanotube-epoxy. *Polymer* (44):5893-5899, 2003.
- [10] L. Wang, ZM. Dang. Carbon nanotube composites with high dielectric constant at low percolation threshold. *Appl Phys Lett* (87): 042903-3, 2005.
- [11] YS. Song, JR. Youn. Influence of dispersion states of carbon nanotubes on physical properties of epoxy nanocomposites. *Carbon* (43):1378-1385, 2005.
- [12] CY. Hong, YZ. You, CY. Pan. A new approach to functionalize multi-walled carbon nanotubes by the use of functional polymers. *Polymer* (47):4300-4309, 2006.
- [13] JF. Shen, WS. Huang, LP. Wu, YZ. Hua and MX. Ye. Study on amino-functionalized multiwalled carbon nanotubes. *Mater Sci Eng A* (464):151-156, 2007.
- [14] T. Saito, K. Matsushige and K. Tanaka. Chemical treatment and modification of multi-walled carbon nanotubes. *Phys B* (323):280-283, 2002.
- [15] SM. Yuen, CM. Ma, YY. Lin, HC. Kuan. Preparation, morphology and properties of acid and amine modified multiwalled carbon nanotube/polyimide composite. *Compos Sci Technol* (67):2564-2573, 2007.
- [16] F. Wang, JW. Wang, SQ. Li and J. Xiao. Dielectric properties of epoxy composites with modified multiwalled carbon nanotubes. *Polym Bull* (63):101-110, 2012.
- [17] CW. Nan. Physics of inhomogeneous inorganic materials. *Prog Mater Sci* (37):1-116, 1993.
- [18] C. Brosseau, F. Boulic, P. Queffelec, C. Bourbigot, YL. Mest. Dielectric and microstructure properties of polymer carbon black composites. *J Appl Phys* (81):882-891, 1997.
- [19] S. Kirkpatrick. Percolation and conduction. *Rev Mod Phys* (45):574-588, 1973.
- [20] CW. Nan, L. Liu, N. Cai, J. Zhai, Y. Ye, YH. Lin et al. A three-phase magnetoelectric composite of piezoelectric ceramics, rare-earth iron alloys, and polymer. *Appl Phys Lett* (81):3831-3833, 2002.
- [21] C. Huang, QM. Zhang. Enhanced dielectric and electromechanical responses in high dielectric constant all-polymer percolative composites. *Adv Funct Mater* (14): 501-506, 2004.
- [22] AV. Goncharenko. Generalizations of the Bruggeman equation and a concept of shape-distributed particle composites. *Phys Rev E* (68):041108, 2003.
- [23] C. Huang, QM. Zhang, G. deBotton, K. Bhattacharya. All-organic dielectric-percolative three-component composite materials with high electromechanical response. *Appl Phys Lett* (84):4391-4393, 2004.
- [24] C. Huang, QM. Zhang, YL. Jiang, R. Manese. Colossal dielectric and electromechanical responses in self-assembled polymeric nanocomposites. *Appl Phys Lett* (87):182901, 2005.
- [25] Y. Lin, J. Wang, L. Jiang, Y. Chen, CW. Nan. High permittivity Li and Al doped NiO ceramics. *Appl Phys Lett* (85):5664, 2004.
- [26] Q. Chen, P. Du, L. Jin, WJ. Weng, GR. Han. Percolative conductor/polymer composite films with significant dielectric properties. *Appl Phys Lett* (91):022912, 2007.
- [27] JW. Wang, QD. Shen, HM. Bao, CZ. Yang. Microstructure and dielectric properties of p(vdf-trfe-cfe) with partially grafted copper phthalocyanine oligomer. *Macromolecules* (38):2247-2252, 2005.
- [28] ZM. Dang, SH. Yao, HP. Xu. Effect of tensile strain on morphology and dielectric property in nanotube/polymer nanocomposites. *Appl Phys Lett* (90):012907, 2007.
- [29] K. Ahmad, W. Pan, SL. Shi. Electrical conductivity and dielectric properties of multiwalled carbon nanotube and alumina composites. *Appl Phys Lett* (89):133122, 2006.
- [30] SI. Lee, Y. Song, TW. Noh, XD. Chen, JR. Gaines. Experimental observation of nonuniversal behavior of the conductivity exponent for three-dimensional continuum percolation systems. *Phys Rev B* (34):6719-6724, 1986.